Spin-Flip Reaction of Re + CH_4—A Relativistic Density Functional Theory Investigation

Jia Li, Xian-Yang Chen, Yi-Xiang Qiu, and Shu-Guang Wang*

School of Chemistry and Chemical Technology, Shanghai Jiao Tong University, 200240 Shanghai, China

Received: April 3, 2009; Revised Manuscript Received: May 13, 2009

To explore the reaction mechanisms of methane dehydrogenation by gas-phase Re atom, the sextet, quartet, and doublet potential energy surfaces have been performed using density functional theory (DFT) and zero-order regular approximation relativistic corrections at the PW91/TZ2P level. The minimum energy reaction path is found to proceed through the following steps: ^{6}Re + CH_4 → $ReCH_4$ (^{6}**1**) → H_3CReH (^{4}**2**) → ^{4}**TS2/3** → H_2CReH_2 (^{4}**3**) → ^{2}**TS3/4** → $HCReH_3$ (^{2}**4**). Also, the reaction path involves the spin inversion twice in the different reaction steps. To better understand the spin inversion processes, the low energy crossing point is determined with the help of the density functional fractional occupation number approach. The first spin inversion, from the sextet state to the quartet state, makes the activation of the C—H bond energetically spontaneous. The second transition from the quartet state to the doublet state facilitates the cleavage of the second C—H bond, lowering the barrier from 186.1 to 24.2 kJ/mol. The overall reaction is calculated to be exothermic by 149.8 kJ/mol, and the final products in three spin states are investigated by NBO analysis, to compare the Re—C bonds and the C—H bonds.

1. Introduction

During the past decades, the C—H bond activation of small alkanes in various cases by transition-metal (TM) atoms and ions has been extensively studied both experimentally[1] and theoretically[2] due to the potential economic and environmental significance and considerable fundamental interest. Methane is the simplest hydride of carbon and the alternative precursor in organic synthesis. However, the activation of the C—H bond in methane is a unique challenge among the hydrocarbons due to its large bond energy[3] (the C—H bond energy in methane is about 440 kJ/mol). The energy to activate a methane molecule can be substantially reduced by catalysts, and among the catalysts, the TM complexes have a higher potential than others.[4]

Comparing with the reaction between TM complexes and methane, the reaction between the naked TM atoms and the methane can provide a simpler model system to study substituent effects on the C—H activation. Fortunately, it has already been discovered by Andrews and co-workers that many atomic TM atoms are capable of activating C—H bonds.[5−8] Many matrix isolation infrared spectroscopic experiments have been carried out for a series of TM atom (from group III to group VIII[6] and a few actinide atoms, Th[7] and U[8]) + CH_4 systems. In all of these works, there are always two issues as to how various TM atoms can react with CH_4 and what the reaction mechanisms in the catalytic processes are. These investigations showed that there are very different reaction mechanisms between the late TM atoms (from group VI to group VIII) and the early ones (from group III to group V and actinide). The late TMs may form $HC{\equiv}MH_3$, whereas the early ones may form $H_2C{=}MH_2$.

Some theoretical research has been published concerning the reactions of TMs with a CH_4 molecule. However, most of this research has been focused on the calculations of frequencies to compare with the experimental results.[9] So far, there are only a few theoretical works that have been done regarding the detailed reaction mechanisms.[10] The difficulty of theoretical investigation in reaction mechanism with heavier TMs is due to correlation effects and relativistic effects. For another difficulty, most of the series of actions occur on several potential energy surfaces (PESs) of different spin symmetries, comprising a variety of cases, which still require formidable theoretical and computational efforts. Much of the discussion of "multiple-state reactivity"[11] has remained qualitative because standard computational methods did not allow for the easy location of crossing points for these processes. Therefore, it is hard to characterize the minimum energy crossing point (MECP) between two different spin symmetric PESs. In this study, we have chosen a simple multiple-state reaction to study how to locate the MECP.

To our knowledge, a recent experimental report of Re + CH_4 was given by Andrews and co-workers,[12] who formed the trihydrido methylidyne complex $HC{\equiv}ReH_3$ in excess argon. These workers also computed B3LYP energies, frequencies, and structures to support their assignment to this lowest energy product. In the reaction, the ground states of the reactant Re atom and the final product are the sextet and doublet states, respectively. So, the respective reaction steps are bound to involve transitions between multielectronic states of different spin multiplicities. In this kind of reaction, there is a difficult question as to how to deal with the crossing point in different states. In Born—Oppenheimer approximation processes, the spin inversion occurs by nonadiabatic coupling over a $3N$-7 dimensional crossing seam of two PESs with different symmetries. It should be satisfied by two conditions: One is to obey the Franck—Condon principle, that is (e.g., ^{1}A and ^{3}B two different symmetries), $E(^1\mathrm{A}) = E(^3\mathrm{B})$ at the same point; the other one is that the crossing point should be the lowest point energetically on the crossing seam. Aiming at this case, the common procedure[10a,b,13] is to simultaneously calculate the two energies of different electronic positions and/or spin symmetries for a given molecular structure and the two gradients. Then, these output data are explicitly processed by an interfaced subroutine, which approaches the MECPs step by step. In this study, we will apply a technically simple approach[14] to determine a low energy crossing point (LECP) on the crossing seam of the two PESs of different symmetry, as a good approximation to the

* Corresponding author.

10.1021/jp9030738 CCC: $40.75
Published on Web 07/02/2009

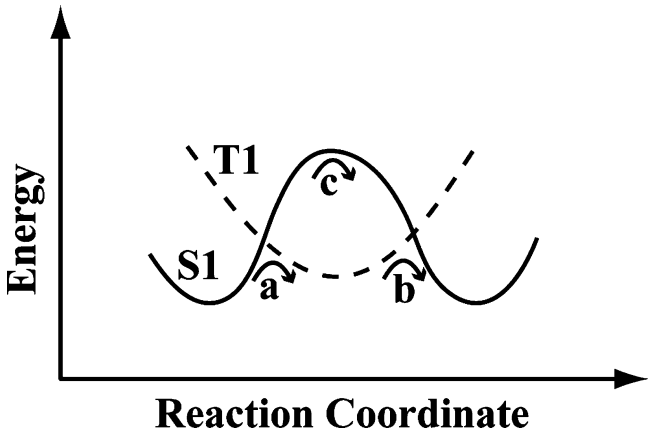

Figure 1. Schematic PES (energy of two states S1 and T1 of different electronic symmetries vs reaction coordinate). (a and b) Transitions with high Boltzmann and low nonadiabatic transition factors. (c) Transition with low Boltzmann and high adiabatic transition factor.[14]

MECP. LECP regions of two PESs of different spin or position symmetry may easily be reached by thermal activation, and that may outbalance a low nonadiabatic transition probability (see Figure 1). The approximate density functional (DF) self-consistent field (SCF) procedure with fractional orbital occupation numbers (FONs) is sufficient for most cases.

To gain systematic insight into the mechanism of the reaction of third-row TM atoms with methane, we present here a theoretical study on the reaction:

$$Re + CH_4 \rightarrow H_3CReH \rightarrow H_2CReH_2 \rightarrow HCReH_3$$

and we determine the energies and structures of the LECPs between two PESs of different spin multiplicities in the reaction pathway to better understand the spin inversion processes. The effect of these crossing points on the energy barriers of different reaction steps is analyzed. The carbon−metal triple bond of the final product has been investigated due to its versatile chemistry and catalytic activities.[15]

2. Computational Details

All calculations were performed using relativistic density functional theory (DFT) program of the Amsterdam DF (ADF2007) package initially develop by Baerends et al.[16] In this work, the DF used was based on the model, the Vosko−Wilk−Nusair (VWN)[17] local spin density correlated potential, and the gradient corrections of the exchange correlation of Perdew and Wang (PW91).[18] The frozen-core approximation was adopted for C ($1s^2$) and Re ($1s^2-4d^{10}$). The core electrons were calculated by the accurate relativistic Dirac−Slater method[19] and then transferred unchanged into the molecules. The valence orbitals of C, Re, and H used triplet-ζ Slater type orbital (STO) with two additional d/f or p/d (for H) polarization function STO basis set (TZ2P).[20] The relativistic corrections were carried out by the zero-order regular approximation, that is, the ZORA method.[21] Equilibrium and transition state structures were fully optimized. Harmonic frequencies were calculated by numerical differentiation of the energy gradients. The vibrational zero point energy (ZPE) corrections were based on the corresponding frequency calculation.

To analyze reaction path characters, the minimum energy path was followed in both directions (forward and backward) using the intrinsic reaction coordinate (IRC)[22] at the level of PW91/TZ2P with ZORA relativistic corrections, on the transition state located at the same theoretical level. An NBO analysis[23] was performed (PW91-DFT level, SDD,[24] and 6-31 g*[25] basis sets for the metal and the other atoms, respectively) using Gaussian03[26] for further elucidation.

TABLE 1: Energy Differences[a] between Ground and Excited Electronic States of Re

state	chosen Slater determinate	PW91 (TZ2P)	ZORA + PW91 (TZ2P)	expt
^6S	$\|(6s)^2(5d_0)^1(5d_{\pm1})^2(5d_{\pm2})^2\|$	0	0	0
^6D	$\|(6s)^1(5d_0)^2(5d_{\pm1})^2(5d_{\pm2})^2\|$	66.9	123.0	99.2
^4G	$\|(6s)^2(5d_0)^2(5d_{+1})^1(5d_{\pm2})^2\|$	98.7	130.1	125.3

[a] Relative energies in kJ/mol with respect to Re(^6S).

TABLE 2: ZPE-Corrected Energies Relative to Re (^6S) + CH_4 (kJ/mol) of Various Compounds and Transition States

species	sextet	quartet	doublet
$Re + CH_4$	0	130.1	258.2
1	−4.2		
PCP1	77.3	77.3	
TS1/2	111.3		
2	−36.4	−61.1	−0.4
TS2/3	123.8	−19.7	18.0
3	63.6	−94.1	−83.3
PCP2		−73.4	−73.4
TS3/4	225.5	92.0	−69.9
4	184.9	51.5	−149.8

3. Results and Discussion

The excited state energies relative to the ground state of the Re atom are shown in Table 1. Table 2 presents the ZPE-corrected energies of various compounds and transition states in the doublet, quartet, and sextet state reaction paths relative to Re (^6S) + CH_4. Table 3 presents the NBO and frequencies analysis in the final products $HCReH_3$ in three spin states. The PESs of the reaction $Re + CH_4 \rightarrow HCReH_3$ in the doublet, quartet, and sextet states are shown in Figure 2 provides the structure parameters of the stationary points of the reaction in three spin . Figure 3states.

3.1. Energy Splitting between Electronic States of Re Atom. According to experimental atomic spectra[27] and spin−orbit averaged values, the lowest excited sextet and quartet states of the Re atom are $5d^66s^1$ (^6D) and $5d^56s^2$ (^4G), which lie above the sextet $5d^56s^2$ (^6S) ground state by 99.2 and 125.3 kJ/mol, respectively. The calculated excitation energies of Re atom are shown in Table 1. Because of the shortage of present-day DFT for representing atomic degenerate densities, we used Baerends method[28] to evaluate the ground, first, and second excited states of Re. The lowest energy of Re (^6S) obtained for the occupation of the d orbital is $(6s)^2(5d_0)^1(5d_{\pm1})^2(5d_{\pm2})^2$. The lowest energies of the ^6D and ^4G states obtained are $(6s)^1(5d_0)^2(5d_{\pm1})^2$-$(5d_{\pm2})^2$ and $(6s)^2(5d_0)^2(5d_{+1})^1(5d_{\pm2})^2$, respectively. There are s → d and d → d electron promotions in the excitations of ^6D and ^4G from ^6S, respectively. As shown in Table 1, the nonrelativistic calculations underestimate the excitation energies of ^6D and ^4G from ^6S by 32.3 and 26.6 kJ/mol, respectively. After relativistic corrections, the excitation energy of ^4G from ^6S is only overestimated 4.8 kJ/mol as compared to experiments. However, the relativistic calculations still overestimate the excited energy of ^6D from ^6S by 23.8 kJ/mol. It is well-known that relativistic effects stabilize the s electron and destabilize the d electron. When one s electron is excited to the d orbital, the relativistic effects play a very important role. Therefore,

TABLE 3: NBO and Frequency Analysis of the Final Products $HCReH_3$ in the Three States

property	HC≡OReH$_3$ (doublet)	HC═ReH$_3$ (quartet)	HC−ReH$_3$ (sextet)
q(H)[a]	0.22	0.20	0.17
q(C)[a]	−0.20	−0.33	−0.46
q(Re)[a]	0.36	0.46	0.56
q(H)[a]	−0.07 × 2, −0.25	−0.12, −0.16, −0.04	−0.09 × 3
H[b]	$1s^{0.78}$	$1s^{0.80}$	$1s^{0.83}$
C[b]	[core]$2s^{1.27}2p^{2.92}$	[core]$2s^{1.42}2p^{2.89}$	[core]$2s^{1.51}2p^{2.93}$
Re[b]	[core]$5d^{5.90}6s^{0.77}$	[core]$5d^{5.75}6s^{0.78}$	[core]$5d^{5.63}6s^{0.76}$
H (×3)[b]	$1s^{1.06}$ × 2, $1s^{1.24}$	$1s^{1.12, 1.16, 1.04}$	$1s^{1.09}$
C−H character[c]	68.3% s, 31.7% p	62.2% s, 37.8% p	61.0% s, 38.8% p
Freq$_{C-H}$[d]	3195.9/(3102)[e]	3073.5	3096.1
EBO$_{C-Re}$	2.80	1.90	0.93
Freq$_{C-Re}$[d]	1078.9/(1049)[e]	845.6	587.7

[a] Natural charge. [b] Natural electron configuration. [c] s and p character percent in the C−H bonds. [d] Frequencies are in cm^{-1}. [e] The values in brackets are the experimental results in ref 12.

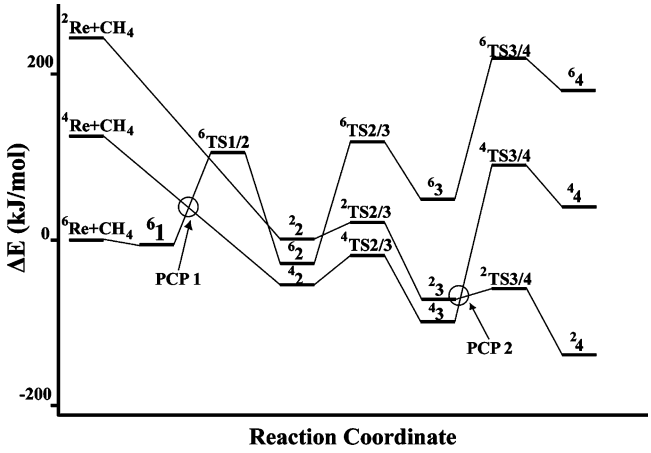

Figure 2. PESs of the reaction Re + CH_4 → $HCReH_3$ in the sextet, quartet, and doublet states, respectively.

we think PW91/TZ2P with the ZORA correction is suitable to reproduce the various electronic states of the Re atom. In this study, we will use the ZORA-PW91 method at the TZ2P level to describe the reactive mechanisms of the Re/CH_4 system.

3.2. Reaction Mechanism in the Doublet State Re (^{2}D) and Quartet State Re (^{4}G). The ground state of the Re atom is ^{6}S ($5d^5 6s^2$); however, the experimental observed ground state of $HCReH_3$ is an electronic doublet state. As seen in Figures 2 and 3, similarly to Cr/W + CH_4[6b] and Os^+ + CH_4[10a] reactions, the mechanisms are possible for Re (^{2}D) + CH_4, which can be called insertion mechanisms. At the initial reaction step, M(M^+) inserts into one C−H bond of CH_4 and yields initially a hydridomethyl complex, H_3CMH, followed by the activation of a second C−H bond. In this case, the Re attacks one of the C−H bonds of CH_4, and an intermediate H_3CReH (^{2}**2**) is spontaneously formed without any barrier. In the intermediate, the Re−H and Re−C bond distances are 1.64 and 2.01 Å. The stabilization energy of the intermediate ^{2}**2** is 258.6 kJ/mol lower than that of the reactants Re (^{2}D) + CH_4.

From the intermediate ^{2}**2**, the reaction proceeds to produce the transition state ^{2}**TS2/3** along with the activation of the second C−H bond. The second C−H bond in ^{2}**TS2/3** slightly elongates to 1.17 Å, while the Re−C bond slightly shrinks by 0.07 Å as compared to that in ^{2}**2**. IRC calculations confirmed that the transition state ^{2}**TS2/3** is connected to the intermediate H_2CReH_2 (^{2}**3**) in the forward direction. The barrier height and exothermicity of the ^{2}**2** → ^{2}**3** reaction step are 18.4 and 82.9 kJ/mol, respectively. From ^{2}**3**, the reaction proceeds to produce $HCReH_3$ (^{2}**4**) via the transition state ^{2}**TS3/4** with 13.4 kJ/mol barrier and releasing energy about 66.5 kJ/mol. To summarize, one can see that the activation of the second C−H bond and of the third C−H bond, with barriers of 18.4 and 13.4 kJ/mol, respectively, are the rate-determining steps on the whole doublet reaction path. The whole reaction on this path is exothermic by 408.0 kJ/mol.

Next, let us turn to the quartet reaction path. Similar to that of the doublet path, the first step of the reaction on the quartet path is the formation of the hydridomethyl intermediate H_3CReH (^{4}**2**), which is a barrierless process. We have undertaken a number of attempts to look for the corresponding complex in these states but failed to find one. The reason may be explained as follows: If the Re inserting into the C−H bond forming a hydridomethyl complex crossing TS needs about 111.3 kJ/mol as in ground state Re (^{6}S), the excited Re (^{2}D) and Re (^{4}G) with higher potential may give enough energy to overcome their activation energy of TS coming down to the intermediate H_3CReH. So, in this process, they were shown without any barrier. The Re···CH_4 complexes **1** are little more stable than the reactants but higher than the followed intermediates **2**, so there is no stop in the process. After ^{4}**2** is formed, one can see that the reaction processes on the quartet path are the same as those on the above-described doublet path.

The intermediate ^{4}**2** has a quite high stabilization by 191.2 kJ/mol relative to the reactants Re (^{4}G) + CH_4. As shown in Figure 3, the second C−H bond length in the transition state ^{4}**TS2/3** is 0.4 Å longer than that in ^{2}**TS2/3**. The Re−C and C−H bond lengths in the final product $HCReH_3$ (^{4}**4**) are 0.12 and 0.01 Å longer than those in ^{2}**4**. From the geometry differences, we can know that $HCReH_3$ in doublet is more stable than that in quartet. On the quartet reaction path, the activation of the third C−H bond with barriers of 186.1 kJ/mol is much larger than that of doublet. The whole reaction on quartet path is exothermic by 78.6 kJ/mol.

3.3. Reaction Mechanism in the Sextet State Re (^{6}S). The ground state of the Re atom is its sextet state ($5d^5 6s^2$), which lies 130.1 and 258.2 kJ/mol below the lowest quartet and lowest doublet states, respectively. Different from that of the quartet and doublet paths, the first step of reaction on the sextet path is the formation of the electrostatic complex (^{6}**1**), which is 4.2 kJ/mol below the reactants Re (^{6}S) + CH_4. In the complex (^{6}**1**), the Re−C bond length is 4.04 Å. Then, the first C−H bond of methane adds to the metal to form the intermediate H_3CReH (^{6}**2**), through the transition state ^{6}**TS1/2**. This step is exothermic by 32.2 kJ/mol, with a barrier of 115.5 kJ/mol. In the transition state ^{6}**TS1/2**, the first C−H and Re−C bond lengths are 1.47 and 2.25 Å, respectively. After ^{6}**2** is formed, one can see that the reaction processes on the sextet path are the same as those on the above-described doublet and quartet paths. In the final

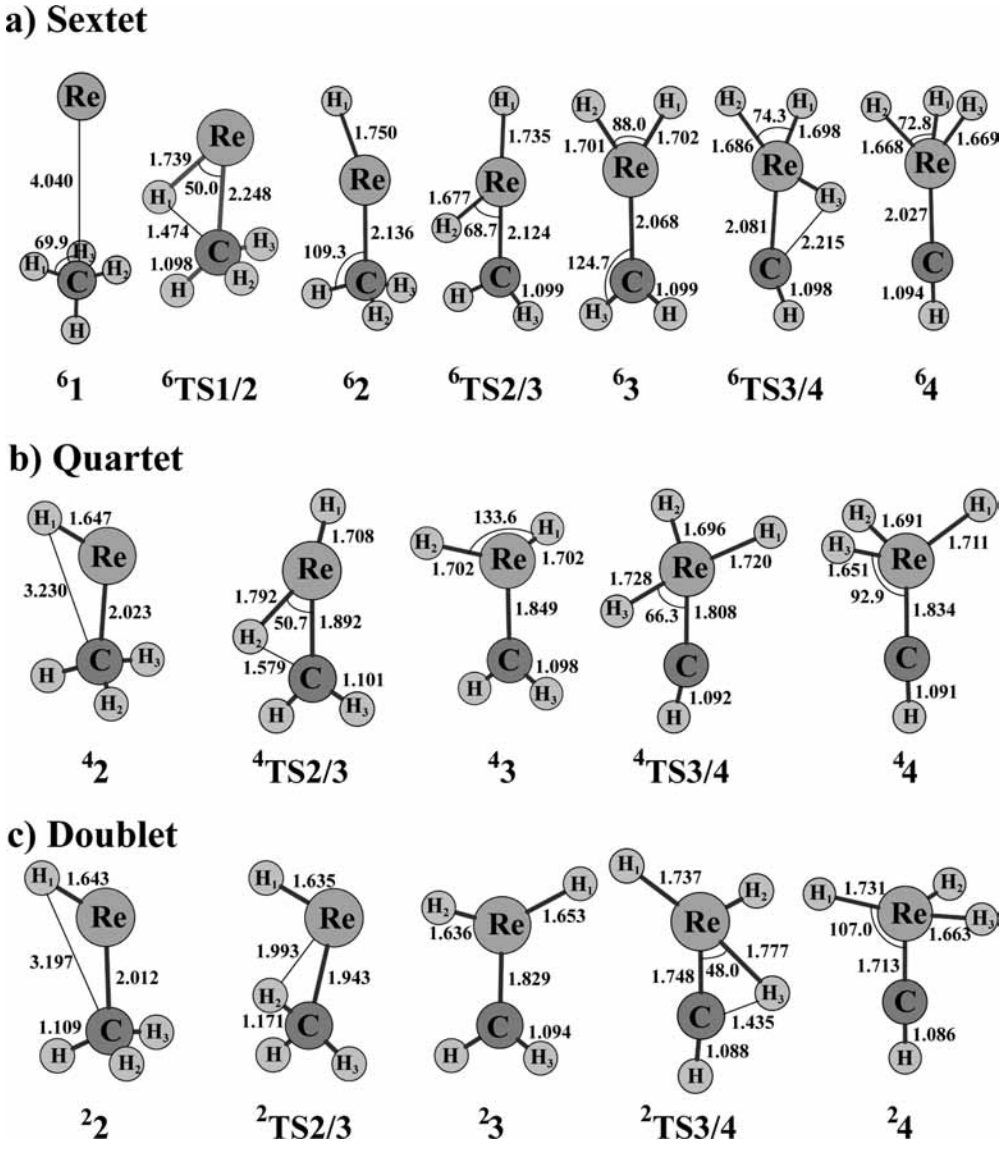

Figure 3. Optimized geometries for the stationary points of the reaction Re + CH_4 → $HCReH_3$ in the (a) sextet, (b) quartet, and (c) doublet states (bond lengths are in Ångstroms, and bond angles are in degrees).

product $HCReH_3$ (^{6}**4**), the Re−C bond length is 0.2 and 0.32 Å longer than those in ^{4}**4** and ^{2}**4**, respectively. On the sextet pathway, the potential energy of the final product $HCReH_3$ (^{6}**4**) is 133.4 and 334.7 kJ/mol higher than those of ^{4}**4** and ^{2}**4**, respectively. The activations of the second C−H bond and the third C−H bond, with very high barriers of 160.2 and 161.9 kJ/mol, respectively, are the slowest steps on the three reaction paths.

3.4. Spin Crossing and the Possible Overall Reaction Path. From the above discussion, we can see that the minimum energy PES is not fixed on one of these three PESs. For example, the sextet PES has the lowest energy in the reactants Re (^{6}S) + CH_4, but the barrier of the first C−H activation is as high as 115.5 kJ/mol, and the overall reaction on the sextet path has an endothermicity of 184.9 kJ/mol. These results contradict the spontaneous dehydrogenation of methane by Re observed experimentally. Thus, the crossing of adiabatic surfaces of different spin is involved in the processes of the reaction. On the other hand, it is well-known that TM-mediated reactions very often occur on more than one adiabatic PES. Some experimental and theoretical evidence has been shown for the systems that include 3d, 4d, and some 5d TMs.[29]

As shown in Figure 2, the minimum energy reaction path requires several possible spin crossings. First, the reaction may start with the formation of the complex ^{6}**1** on the sextet PES. Then, the sextet surface should cross the quartet surface somewhere between ^{6}**1** and ^{6}**TS1/2**, and the reaction should proceed on the quartet surface to form ^{4}**2**, ^{4}**TS2/3**, and ^{4}**3**. After ^{4}**3** is formed, the reaction may jump to the doublet PES between **3** and **TS3/4** since ^{4}**TS3/4** is 161.9 kJ/mol above ^{2}**TS3/4** and the final product ^{2}**4** on the doublet PES is thermodynamically much favored than that on the quartet PES. So, the reaction may jump to the doublet PES. It only needs 24.2 kJ/mol to pass the transition state ^{2}**TS3/4** and form the final product ^{2}**4**. To summarize, the minimum energy pathway may proceed as ^{6}Re + CH_4 → $ReCH_4$ (^{6}**1**) → H_3CReH (^{4}**2**) → ^{4}**TS2/3** → H_2CReH_2 (^{4}**3**) → ^{2}**TS3/4** → $HCReH_3$ (^{2}**4**). If the reaction starts on the sextet PES and ends on the doublet PES, the overall reaction would be exothermic by 149.8 kJ/mol.

3.5. Crossing Points between the PESs of Different Multiplicities. To better understand the spin inversion processes described above, it is instructive to locate the LECP1 between the sextet and the quartet PESs and the LECP2 between the

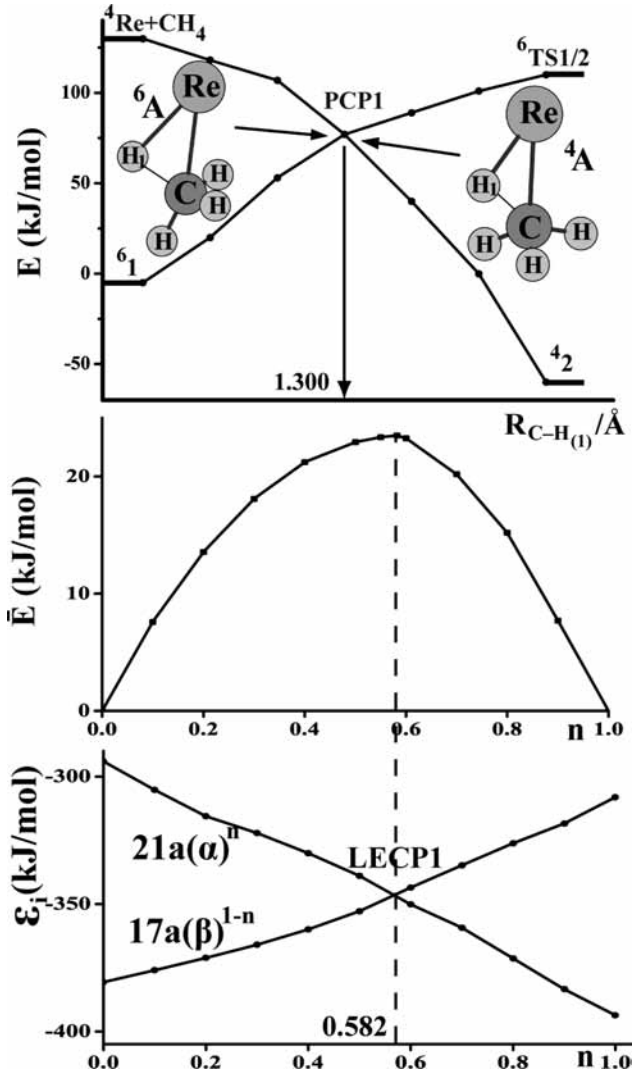

Figure 4. $ReCH_4$ (^{6}**1**) → H_3CReH (^{4}**2**) rearrangement. Top: Optimized energy curves E along reaction coordinate $R_{C-H(1)}$. Middle and bottom: Ensemble energy $\bar{E}$ and orbital energies ε_i of 17a(β)$^{1-n}$ and 21a(α)^n for mixed ensemble $(1-n)(^4A) + n(^6A)$, when varying the FON n with optimized partial structure.

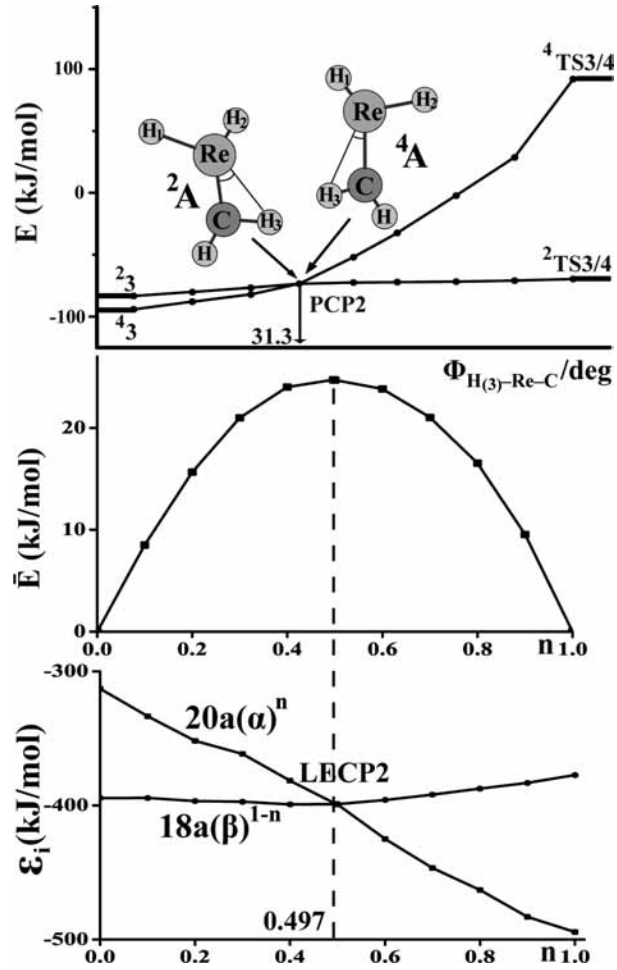

Figure 5. ^{4}**3** → ^{2}**TS3/4** rearrangement. Top: Optimized energy curves E along reaction coordinate $\Phi_{H(3)-Re-C}$. Middle and bottom: Ensemble energy $\bar{E}$ and orbital energies ε_i of 18a(β)$^{1-n}$ and 20a(α)^n for mixed ensemble $(1-n)(^2A) + n(^4A)$, when varying the FON n with optimized partial structures.

quartet and the doublet PESs on the reaction pathway. The method has been described in ref 14 in detail.

From the study of the LECP1, there is the activation of the C−H bond on the pathway, which proceeds to produce the H_3CReH (^{4}**2**) via the crossing point 1 (see Figure 2). The C−$H_{(1)}$ bond length varies significantly from the initial to the final state. Then, the C−$H_{(1)}$ bond is chosen as a reaction coordinate, and the other geometric parameters are optimized in each steps along the C−$H_{(1)}$, changing to get a minimum potential path in the 3N-7 dimension. The scan of the bond length yields two energy troughs, for the sextet and quartet states going up from the minimum at 1.07 Å, which is the value in the CH_4 geometry. As seen from Figure 4, there is a "projected crossing point" (PCP1) at $R_{C-H(1)}$ = 1.300 Å with $E(^6A) = E(^4A)$. The two electronic states have the same, comparatively low, energy at PCP1 but less or more different partial structures except for $R_{C-H(1)}$. We should note that at the PCP1 Franck−Condon principle is not satisfied. Now, we use the DFT-FON procedure to find the LECP1. Beside the $R_{C-H(1)}$, which is fixed, all other geometric parameters are optimized along with the optimization of fractional occupation number n on orbitals 17a(β)^n and 21a(α)$^{1-n}$ for the state ensemble. When n increases, the orbital 17a(β)^n shifts down and 21a(α)$^{1-n}$ goes up. At point n = 0.582, the two orbitals become equal, and the DFT "aufbau principle" is satisfied again (Figure 4). The LECP1 is reached. Detailed structures of LECP1 are shown in Figure 6. With this structure, we can calculate the individual pure-state energies of ^{6}A and ^{4}A. The energy difference of ^{6}A and ^{4}A is only 0.6 kJ/mol. At this point, the Franck−Condon principle is satisfied. If checking the electronic configurations of the LECP1 in the sextet and quartet states, we can find that both of these two states satisfy the "aufbau principle", which should always be obeyed in DFT.[30] If the electron occupies the 17a(β)^1 position, the 21a(α)^0 is higher than the former orbital; if the electron occupies the orbital 21a(α)^1 position, then the orbital 17a(β)^0 will be higher than the former one. There is not always an empty orbital below the occupied orbital. Normally, there is an empty orbital below the occupied orbital in the excited state. So, this is the typical multiconfiguration case in DFT here.

For the LECP2 between the quartet and the doublet states, we investigated it using the ∠$H_{(3)}$ReC angle as the reaction coordinate. The two electronic states ^{4}A and ^{2}A have the same energy at the PCP2 (∠$H_{(3)}$ReC = 31.3°). After the optimization with the FON approach (see Figure 5), we get the structures of the LECP2 (see Figure 6). The individual pure-state energies of the LECP2 (∠$H_{(3)}$ReC = 31.3°, n = 0.497) in quartet and doublet states are −2720.3 and −2719.9 kJ/mol, respectively.

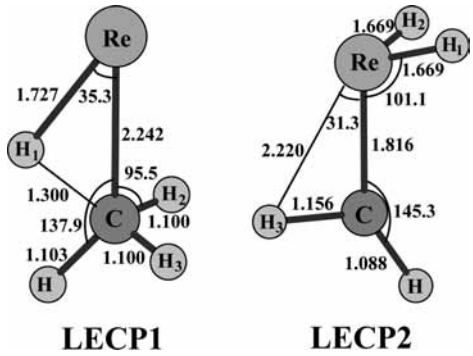

Figure 6. Structural parameters of two LECPs (bond lengths are in Ångstroms, and bond angles are in degrees).

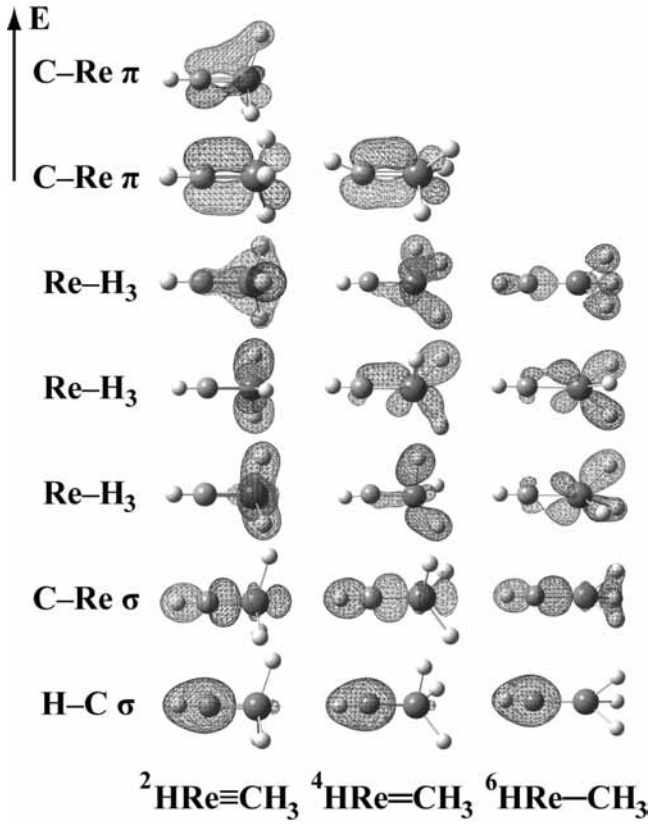

Figure 7. Seven, six, and five highest molecular orbitals in doublet, quartet, and sextet states are calculated, respectively. Molecular orbitals from top to bottom are degenerate π, degenerate π, degenerate R−H_3, degenerate Re−H_3, Re−H_3, C−Re σ, and H−C σ, respectively.

There is only a 0.4 kJ/mol difference in energy between ^{4}A and ^{2}A, which satisfies the Franck−Condon principle.

If we use a normal procedure[31] to treat such a system, for example, at the LECP2, along the reaction path, we optimize the ^{4}A state and with this structure single point calculate the ^{2}A state energy. The two potential curves will cross each other; at the crossing point, the energy is higher by about 60−70 kJ/mol than our result. We optimize the ^{2}A state and with this structure single point calculate the ^{4}A state energy. There is no crossing found anymore. So, with the DFT-FON procedure, more reasonable reaction mechanisms can be achieved.

3.6. Structure and Bonding. The structures of the final products in three states are collected in Figure 3. The doublet $HCReH_3$ structure is essentially the same as that reported by Cho and Andrews at the B3LYP level of theory.[12] The C−Re bond lengths range from 1.713 (doublet) and 1.834 (quartet) to 2.027 Å (sextet), and the C−Re bonds can be considered triple bonds, double bonds, and single bonds, respectively. The conclusion can be interpreted by the effective bond order (EBO), which is estimated from the orbital occupancies and are listed in Table 3. The EBO thus calculated for the doublet $HCReH_3$ triple bond is 2.80, which is higher than those for the quartet (1.90) and the sextet (0.93) states. The several highest occupied molecular orbitals for the final product in the three states are shown in Figure 7. The two degenerate π orbitals that make up part of the triple bond are highest in the doublet state. There is only one or none degenerate π orbital in the quartet and sextet states, respectively. These orbitals in the three states have similar shapes. In addition, the frequencies of the Re−C bond are 1078.9, 845.6, and 587.7 cm^{-1} in the doublet, quartet, and sextet states, respectively.

It is also significant that the final product $HCReH_3$ in the doublet state is polarized quite differently from those in the quartet and sextet states. Natural charges for the atoms in order, left to right, for these three states, respectively, are 0.22, −0.20, 0.36, −0.13 (×3) and 0.20, −0.33, 0.46, −0.11 (×3) and 0.17, −0.46, 0.56, and −0.09 (×3). This polarization affects the C−H bond and reduces the s character (68.3%) in the doublet state. It is noteworthy that the C−H frequency of the final product in the doublet state is about 120 and 100 cm^{-1} higher than those in the quartet and sextet states, respectively.

4. Conclusions

DF calculations have been performed to investigate the mechanism of methane dehydrogenation by Re atom. The sextet, quartet, and doublet PESs of the reaction have been explored. We may draw the following conclusions from the present calculations.

1. The minimum energy reaction path is found not to be on one of the three PESs of a certain spin state. Instead, the minimum energy reaction path requires the crossing of two adiabatic surfaces with different spin states in the different reaction steps. Totally, three spin states are involved in the whole reaction. The minimum energy pathway can be described as ^{6}Re + CH_4 → $ReCH_4$ (^{6}**1**) → H_3CReH (^{4}**2**) → ^{4}**TS2/3** → H_2CReH_2 (^{4}**3**) → ^{2}**TS3/4** → $HCReH_3$ (^{2}**4**).

2. The reacting system should change its spin multiplicity two times in the whole reaction processes. The first spin inversion, from the sextet state to the quartet state, occurs in the LECP1, which makes the activation of the first C−H bond energetically spontaneous. After passing this point, the reaction path moves on the quartet PES toward the hydridomethyl complex ^{4}**3**. The second crossing seam exists between ^{4}**3** and ^{2}**TS3/4**, in the region where the third C−H bond of methane is being activated. This spin inversion leads to a decrease in the reductive elimination barrier height from 186.1 to 24.2 kJ/mol. The reaction starts on the sextet PES and ends on the doublet PES, and the overall reaction is calculated to be exothermic by 149.8 kJ/mol.

3. The three final products in different states are investigated by NBO and frequencies analysis. As might be expected, we find the effective triple bond orders of the final products $HCReH_3$ in the doublet state. The EBO values are 2.80, 1.90, and 0.93 of the Re−C bond in the doublet, quartet, and sextet states, respectively, and the $HCReH_3$ in the doublet state has the shortest C−H bond because of the different polarization.

Acknowledgment. We acknowledge financial support by the National Nature Science Foundation of China (No. 20773086).

References and Notes

(1) (a) Llabunde, K. J.; Tanaka, Y. *J. Am. Chem. Soc.* **1983**, *105*, 3544. (b) Billups, W. E.; Konarski, M. M.; Hauge, R. H.; Margrave, J. L. *J. Am.*

Chem. Soc. **1980**, *102*, 7393. (c) Ozin, G. A.; McIntosh, D. F.; Mitchell, S. A.; Garcia-Prieto, J. *J. Am. Chem. Soc.* **1981**, *103*, 1574. (d) Remick, R. J.; Asunta, T. A.; Skell, P. S. *J. Am. Chem. Soc.* **1979**, *101*, 1320. (e) Wang, G.; Chen, M.; Zhou, M. *Chem. Phys. Lett.* **2005**, *412*, 46. (f) Bloomberg, M. R. A.; Siegbahn, P. E. M.; Svensson, M. *J. Am. Chem. Soc.* **1992**, *114*, 6095. (g) Squires, R. R. *Chem. Rev.* **1987**, *87*, 623. (h) Armentrout, P. B.; Beauchamp, J. L. *Acc. Chem. Res.* **1989**, *22*, 315. (i) Eller, K.; Schwarz, H. *Chem. Rev.* **1991**, *91*, 1121. (j) Armentrout, P. B. *Science* **1991**, *251*, 175. (k) Weissharr, J. C. *Acc. Chem. Res.* **1993**, *26*, 213. (l) Bowers, M. T. *Acc. Chem. Res.* **1994**, *27*, 324. (m) Freiser, B. S. *Acc. Chem. Res.* **1994**, *27*, 353. (n) Armentrout, P. B. *Acc. Chem. Res.* **1995**, *28*, 430.

(2) (a) Yoshizawa, K.; Suzuki, A.; Yamabe, T. *J. Am. Chem. Soc.* **1999**, *121*, 5266. (b) Hendrickx, M.; Ceulemans, M.; Gong, K.; Vanquickenborne, L. *J. Phys. Chem. A* **1997**, *101*, 2465. (c) Irikura, K. K.; Goddard, W. A. *J. Am. Chem. Soc.* **1994**, *116*, 8733. (d) Heinemann, C.; Hertwig, R. H.; Wesendrup, R.; Koch, W.; Schwarz, H. *J. Am. Chem. Soc.* **1995**, *117*, 495. (e) Zhang, X. G.; Liyanage, R.; Armentrout, P. B. *J. Am. Chem. Soc.* **2001**, *123*, 5563. (f) Achatz, U.; Beyer, M.; Joos, S.; Fox, B. S.; Niedner-Schatteburg, G.; Bondybey, V. E. *J. Phys. Chem. A* **1999**, *103*, 8200. (g) Sicilia, E.; Russo, N. *J. Am. Chem. Soc.* **2002**, *124*, 1471.

(3) (a) Crabtree, R. H. *Chem. Rev.* **1985**, *85*, 245. (b) Crabtree, R. H. *Chem. Rev.* **1995**, *95*, 987.

(4) (a) Braunstein, P.; Matt, D.; Nobel, D. *Chem. Rev.* **1988**, *88*, 747. (b) Davies, H. M. L.; Beckwith, E. J. *Chem. Rev.* **2003**, *103*, 2861.

(5) (a) Andrews, L.; Citra, A. *Chem. Rev.* **2002**, *102*, 885. (b) Andrews, L. *Chem. Soc. Rev.* **2004**, *33*, 123. (c) Andrews, L.; Cho, H. G. *Organometallics* **2006**, *25*, 4040.

(6) (a) Andrews, L.; Cho, H. G.; Wang, X. F. *Angew. Chem., Int. Ed.* **2005**, *44*, 113. (b) Cho, H. G.; Andrews, L.; Marsden, C. *Inorg. Chem.* **2005**, *44*, 7634. (c) Andrews, L.; Cho, H. G.; Wang, X. F. *Inorg. Chem.* **2005**, *44*, 4834. (d) Cho, H. G.; Wang, X. F.; Andrews, L. *J. Am. Chem. Soc.* **2005**, *127*, 465. (e) Cho, H. G.; Andrews, L. *J. Am. Chem. Soc.* **2005**, *127*, 8226. (f) Cho, H. G.; Andrews, L. *J. Phys. Chem. A* **2006**, *110*, 3886. (g) Roos, B. O.; Lindh, R.; Cho, H. G.; Andrews, L. *J. Phys. Chem. A* **2007**, *111*, 6420. (h) Cho, H. G.; Andrews, L. *Organometallic* **2007**, *26*, 633. (i) Cho, H. G.; Wang, X. F.; Andrews, L. *Organometallic* **2005**, *24*, 2854. (j) Cho, H. G.; Andrews, L. *Organometallics* **2008**, *27*, 1786.

(7) Andrews, L.; Cho, H. G. *J. Phys. Chem. A* **2005**, *109*, 6796.

(8) Lyon, J. T.; Andrews, L.; Hu, H. S.; Li, J. *Inorg. Chem.* **2008**, *47*, 1435.

(9) (a) Lyon, J. T.; Cho, H. G.; Andrews, L.; Hu, H. S.; Li, J. *Inorg. Chem.* **2007**, *46*, 8728. (b) Wang, G. J.; Gong, Y.; Chen, M. H.; Zhou, M. F. *J. Am. Chem. Soc.* **2006**, *128*, 5974. (c) Cho, H. G.; Andrews, L. *J. Phys. Chem. A* **2006**, *110*, 13151.

(10) (a) Zhang, G. B.; Li, S. H.; Jiang, Y. S. *Organometallics* **2003**, *22*, 3820. (b) Guo, Z.; Ke, Z. F.; Phillips, D. L.; Zhao, C. Y. *Organometallics* **2008**, *27*, 181. (c) Carren-Macedo, J.; Harvey, J. N. *J. Am. Chem. Soc.* **2004**, *126*, 5789. (d) de Almeida, K. J.; Cesar, A. *Organometallics* **2006**, *25*, 3407.

(11) (a) Gutlich, P.; Garcia, Y.; Woike, T. *Coord. Chem. Rev.* **2001**, *219*, 839. (b) Gutlich, P.; Garcia, Y.; Goodwin, H. A. *Chem. Soc. Rev.* **2000**, *29*, 419. (c) Harvey, J. N.; Poli, R.; Smith, K. M. *Coord. Chem. Rev.* **2003**, *238*, 347.

(12) (a) Cho, H. G.; Andrews, L. *Organometallics* **2007**, *26*, 4098. (b) Cho, H. G.; Andrews, L. *Inorg. Chem.* **2008**, *47*, 1653.

(13) (a) Domcke, W.; Yarkony, D. R.; Koeppel, H. *Conical Intersections: Electronic Structure, Dynamics and Spectroscopy*; World Scientific: Singapore, 2004. (b) Lorquet, J. C. *Int. J. Mass. Spectrom.* **2000**, *200*, 43. (c) Yarkony, D. R. *J. Phys. Chem.* **1993**, *97*, 4407. (d) Lundberg, M.; Siegbahn, P. E. M. *J. Phys. Chem. B* **2005**, *109*, 10513. (e) Schoeneboom, J.; Thiel, W. *J. Am. Chem. Soc.* **2004**, *126*, 4017. (f) Schwarz, H. *Int. J. Mass. Spectrom.* **2004**, *237*, 75.

(14) Wang, S. G.; Chen, X. Y.; Schwarz, W. H. E. *J. Chem. Phys.* **2007**, *126*, 124109.

(15) (a) Schrock, R. R. *Chem. Rev.* **2002**, *102*, 145. (b) Herndon, J. W. *Coord. Chem. Rev.* **2004**, *248*, 3. (c) Da Re, R. E.; Hopkins, M. D. *Coord. Chem. Rev.* **2005**, *249*, 1396.

(16) (a) Baerend, E. J.; Ellis, D. E.; Ros, P. *Chem. Phys.* **1973**, *2*, 41. (b) Velde, G.; Baerends, E. J. *J. Comput. Phys.* **1992**, *99*, 84. (c) Ziegler, T.; Rauk, A.; Baerend, E. J. *Theor. Chim. Acta* **1977**, *43*, 261.

(17) Vosko, S. H.; Wilk, L.; Nusair, M. *Can. J. Phys.* **1980**, *58*, 1200.

(18) Perdew, J. P.; Chevary, J. A.; Vosko, S. H.; Jackson, K. A.; Pederson, M. R.; Singh, D. J.; Fiolhais, C. *Phys. Rev. B* **1992**, *46*, 6671.

(19) Rosen, A.; Lindgren, I. *Phys. Rev.* **1968**, *176*, 114.

(20) van Lenthe, E.; Baerends, E. J. *J. Comput. Chem.* **2003**, *24*, 1142.

(21) van Lenthe, E.; Baerends, E. J.; Snijders, J. G. *J. Chem. Phys.* **1994**, *101*, 9783.

(22) (a) Deng, L.; Ziegler, T.; Fan, L. *J. Chem. Phys.* **1993**, *99*, 3823. (b) Deng, L.; Ziegler, T. *Int. J. Quantum Chem.* **1994**, *52*, 731.

(23) Reed, A. E.; Curtiss, L. A.; Weinhold, F. *Chem. Rev.* **1988**, *88*, 899.

(24) Andrae, D.; Haeussermann, U.; Dolg, M.; Stoll, H.; Preuss, H. *Theor. Chim. Acta* **1990**, *77*, 123.

(25) Ditchfield, R.; Hehre, W. J.; Pople, J. A. *J. Chem. Phys.* **1971**, *54*, 724.

(26) Frisch, M. J.; Trucks, G. W.; Schlegel, H. B.; Scuseria, G. E.; Robb, M. A.; Cheeseman, J. R.; Montgomery, J. A.; Vreven, T.; Kudin, K. N.; Burant, J. C.; Millan, J. M.; Iyengar, S. S.; Tomasi, J.; Barone, V.; Mennucci, B.; Cossi, M.; Scalmani, G.; Rega, N.; Petersson, G. A.; Nakatsuji, H.; Hada, M.; Ehara, M.; Toyota, K.; Fukuda, R.; Hasegawa, J.; Ishida, M.; Nakajima, T.; Honda, Y.; Kitao, O.; Nakai, H.; Klene, M.; Li, X.; Knox, J. E.; Hratchian, H. P.; Cross, J. B.; Bakken, V.; Adamo, C.; Jaramillo, J.; Gomperts, R.; Stratmann, R. E.; Yazyev, O.; Austin, A. J.; Cammi, R.; Pomelli, C.; Ochterski, J. W.; Ayala, P. Y.; Morokuma, K.; Voth, G. A.; Salvador, P.; Dannenberg, J. J.; Zakrzewski, V. G.; Dapprich, S.; Daniels, A. D.; Strain, M. C.; Farkas, O.; Malick, D. K.; Rabuck, A. D.; Raghavachari, K.; Foresman, J. B.; Ortiz, J. V.; Cui, Q.; Baboul, A. G.; Clifford, S.; Cioslowski, J.; Stefanov, B. B.; Liu, G.; Liashenko, A.; Piskorz, P.; Komaromi, I.; Martin, R. L.; Fox, D. J.; Keith, T.; Al-Laham, M. A.; Peng, C. Y.; Nanayakkara, A.; Challacombe, M.; Gill, P. M. W.; Johnson, B.; Chen, W.; Wong, M. W.; Gonzalez, C.; Pople, J. A. *GAUSSIAN 03*, Gaussian, Inc.: Wallingford, CT, 2004.

(27) NIST Chemistry Webbook, NIST Standard Reference Data Base Number 69, http://physics.nist.gov/PhysRefDate/Handbook/Tables/rheniumtable5.htm.

(28) Baerends, E. J.; Branchadell, V.; Sodupe, M. *Chem. Phys. Lett.* **1997**, *265*, 481.

(29) (a) Russo, N.; Sicilia, E. *J. Am. Chem. Soc.* **2001**, *123*, 2588. (b) Westerberg, J.; Blomberg, M. R. A. *J. Phys. Chem. A* **1998**, *102*, 7303. (c) Sändig, N.; Koch, W. *Organometallics* **1997**, *16*, 5244. (d) Perry, J. K.; Ohanessian, G.; Goddard, W. A. *Organometallics* **1994**, *13*, 1870. (e) de Visser, S. P.; Ogliaro, F.; Harris, N.; Shaik, S. *J. Am. Chem. Soc.* **2001**, *123*, 3037.

(30) Janak, J. F. *Phys. Rev.* **1978**, *18*, 7165.

(31) Koga, N.; Morokuma, K. *Chem. Phys. Lett.* **1985**, *119*, 371.

JP9030738